# Investigation of bound diffusion of ultrafine particles of $Fe^{III}$ hydroxide in a polymeric sorbent by Mössbauer spectroscopy

*V. I. Khromov,[a]* A. S. Plachinda,[b]* S. I. Kamyshanskii,[a] and I. P. Suzdalev[b]*

[a]*D. I. Mendeleev University of Chemical Technology of Russia, 9 Miusskaya pl., 125190 Moscow, Russian Federation. Fax: +7 (095) 200 4204*

[b]*N. N. Semenov Institute of Chemical Physics, Russian Academy of Sciences, 4 ul. Kosygina, 117977 Moscow, Russian Federation. Fax: +7 (095) 938 2156*

Bound diffusion of ultrafine particles of $Fe^{III}$ hydroxide in the pores of a solvated polymeric sorbent has been discovered and investigated by Mössbauer spectroscopy. Particles with diameters of 30 Å $\leq d \leq$ 90 Å were precipitated from an aqueous solution in the pores of the poly(divinylbenzene—ethylstyrene) "Porolas A" sorbent. The Mössbauer spectra obtained at $T > 250$ K (*i.e.*, above the crystallization and glass transition points of the liquid in the pores, *viz.*, water or glycerol) were found to assume the shape of a superposition of broadened and nonbroadened components, which is characteristic of bound diffusion. Experimental data were treated in terms of two alternative models of bound diffusion, *viz.*, in harmonic (Brownian overdamped oscillator) and rectangular potentials. The following values for the parameters of bound diffusion (diffusion coefficient $D$ and diffusion displacement $r$) at room temperature were found: for glycerol, $D = 0.3 \cdot 10^{-9}$; $0.5 \cdot 10^{-9}$ cm$^2$ s$^{-1}$ and $r =$ 0.14; 0.38 Å; for water, $D > 2 \cdot 10^{-8}$ cm$^2$ s$^{-1}$ and $r = 0.22$; 0.45 Å. Unlimited diffusion of particles in the solvated sorbent was not observed. No diffusion of the particles was observed in the dry sorbent.

**Key words:** bound diffusion, ultrafine particles, nanoparticles, Mössbauer spectroscopy, polymeric sorbents.

It is known that the use of Mössbauer spectroscopy made it possible to study the mechanism of diffusion in solids and liquids at the atomic level (see, for example, Refs. 1—9) including some aspects that cannot be studied (or are difficult to study) by macroscopic methods, such as the ratio of continuous and jump diffusion in structurized liquids, correlated diffusion in solids, *etc.* The unlimited diffusion (including that of ultrafine particles in liquids[10—13]), resulting in a general broadening of the Mössbauer line, has been considered in numerous papers. More recently, papers devoted to a more complex sort of motion, namely, bound diffusion (in the microscopic sense, this means that the range of diffusion displacements or jumps is limited to values of $\sim 10^{-10}$ m or less, and the maximum displacements are achieved over small periods of time), have been published. In this case, the shape of the Mössbauer line changes markedly and embodies much information concerning the mechanism and the parameters of the motion.[14—17]

Actually, three groups of objects are currently studied, namely: (1) crystals in which the jumps of atoms are limited to a small region;[18,19] (2) viscous liquids in the region of the glass—crystal transition, in which atoms or small solid-state particles exhibit signs of bound diffusion;[20] (3) small particles in solvated polymer networks.[21—24] These studies border, in some sense, on the studies of intramolecular mobility of macromolecules, polymeric networks, and biopolymers (see, for example, Ref. 25) carried out by Mössbauer spectroscopy (and by Rayleigh scattering of the Mössbauer radiation), since the low-frequency motions of the fragments of these systems also have the character of bound diffusion.

Since there exist grounds for believing that this type of motion is rather frequently encountered, it is of obvious interest to widen the scope of the investigation objects. Therefore, in the present work, to continue our previous studies dealing with the bound diffusion of ultrafine particles in polymer networks of cation exchangers,[21—24] we attempted to detect this diffusion in the pores of a sorbent.

## Experimental

For our studies, we chose the "Porolas A" polymeric sorbent (Russia), which is analogous to «Amberlite XAD-2» (USA). It is a porous granular copolymer of divinylbenzene (70 %) and ethylstyrene (30 %), prepared by suspension polymerization in the presence of a modifying solvent.

Translated from *Izvestiya Akademii Nauk. Seriya Khimicheskaya*, No. 4, pp. 886—895, April, 1996.

1066-5285/96/4504-0841 $15.00 

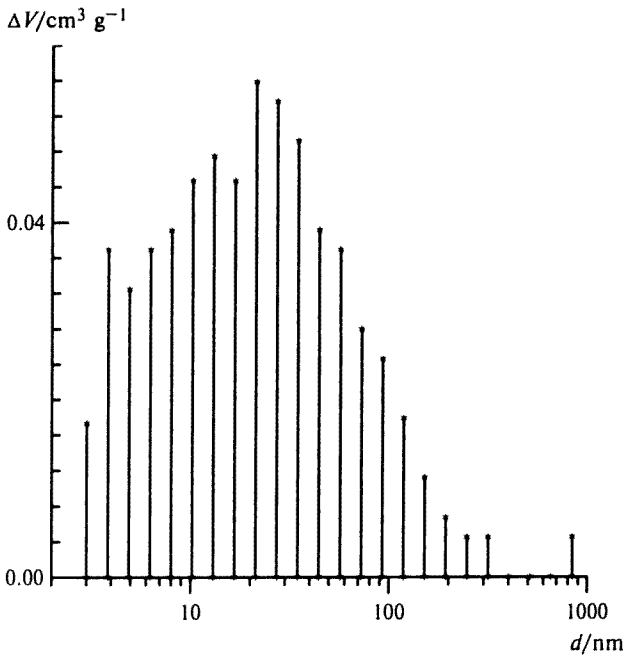


**Fig. 1.** Distribution of the diameters of pores in the sorbent according to the data of mercury porosimetry.

Figure 1 presents the differential diagram of the size distribution of pores obtained by mercury porosimetry (MP). Structural characteristics of the sorbent: overall volume of the pores 0.70 (MP) or 0.88 $cm^3\ g^{-1}$ (hydration), specific surface area 190 (MP) or 323 $m^2\ g^{-1}$ (BET, using benzene adsorption), average diameter of the pores 14.8 (MP) or 10.9 nm (BET).

To impart hydrophilic properties to the sorbent we impregnated it with 2-propanol, which was then washed out with water. Grains of the partially hydrated sorbent of size 1—2 mm were then impregnated with an aqueous solution of $^{57}FeCl_3$ acidified with HCl. After that, to precipitate the particles of iron hydroxide in the pores of the sorbent, the grains were kept for 70 min with vigorous stirring in twofold excess of a 2 *M* solution of KOH (taking into account neutralization of HCl and precipitation of $Fe(OH)_3$).

After the precipitation of the hydroxide, the sample was washed with water (which was replaced five times) for 2 h to pH ≈ 7. The highly concentrated alkaline solution was chosen for the precipitation to ensure that its diffusion flow into a grain is more intense than the counter flow of the iron salt. Visual examination of a grain cut and electron microprobe analysis showed (Fig. 2) that iron hydroxide had precipitated throughout the whole bulk of the grain rather than on its surface (although its concentration increased somewhat along the radius from the center of the grain to the surface).

In the present work, the intensity of the Mössbauer spectrum varied more than 10-fold (due to the variation of the temperature of the measurement and the viscosity of the solvating liquid, and also due to drying of the sample); in other words, a sample that was thin with respect to the Mössbauer $^{57}Fe$ isotope under some conditions became thick under other conditions (the content of the isotope being invariable). Therefore, to avoid too great errors in the measurement of the areas of the spectra, we carried out parallel measurements for the samples prepared using natural iron (2.2 % $^{57}Fe$) and iron

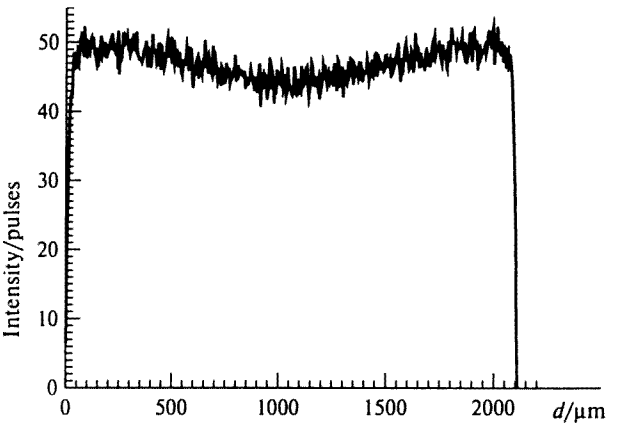


**Fig. 2.** Concentration profile of iron over the diameter of a grain of the sorbent from electron microprobe data.

enriched in the Mössbauer isotope (96 % $^{57}Fe$). For the quantitative analysis of these areas, we used their numerical values obtained with samples that are thin with respect to $^{57}Fe$ and normalized on the basis of the $^{57}Fe$ content.

Hydrated, glycerol-solvated, and dry samples were studied. The so-called glycerol samples were obtained by immersing the hydrated forms into a large excess of anhydrous glycerol (the minor quantity of water that may be present was not determined) followed by keeping them in glycerol in a sealed vessel for 2 days. The viscosity of glycerol with an impurity of water in the pores of the glycerol samples calculated[26] on the arbitrary assumption that there was no selective sorption of the components (*i.e.*, that the glycerol : water ratios in the sorbent pores and in the external equilibrium solution were identical) was 7.7 P. Dry samples were obtained by drying the hydrated forms in a vacuum desiccator over $P_2O_5$ at room temperature. During the studies, the solvated and dry samples were stored in hermetically sealed cells.

## Results and Discussion

The Mössbauer spectrum of the sorbent with iron hydroxide particles recorded at $T = 77$ K (Fig. 3) is a superposition of a quadrupole doublet (*1*) (the isomeric shift with respect to sodium nitroprusside $\delta E_I = 0.70\pm0.05$ mm $s^{-1}$, quadrupole splitting $\Delta E_Q = 0.74\pm0.05$ mm $s^{-1}$) and a broadened sextet (*2*) with a magnetic hyperfine structure (HFS) ($\delta E_I = 0.73\pm0.05$ mm $s^{-1}$, $\Delta E_Q = -0.19\pm0.05$ mm $s^{-1}$, the maximum value for the effective magnetic field at the iron nucleus $H_{max} = 485\pm5$ kOe). This spectrum is typical of ultrafine particles of iron hydroxide in the region of its transition from the antiferromagnetic state to the superparamagnetic or paramagnetic state. The component of the spectrum with resolved magnetic HFS is completely "collapsed" into a quadrupole doublet at $T \approx 250$ K.

If we assume that the precipitated particles have the same nature as those precipitated in sulfocation-exchange membranes[27] and resins,[24] an estimate of the average size of particles based on the expression for the time of their superparamagnetic relaxation $\tau = \tau_0 \exp(KV/kT)$

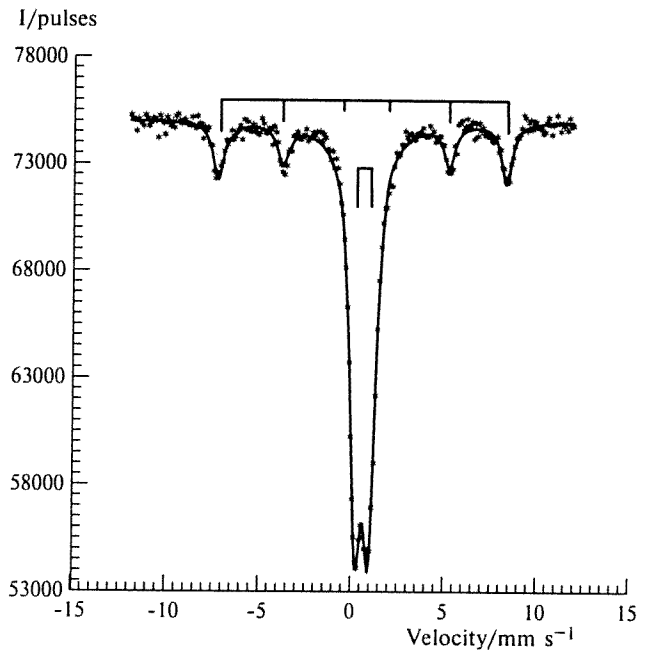


**Fig. 3.** Mössbauer spectrum of the sorbent with $Fe^{III}$ hydroxide particles.

(where K is the constant of magnetic anisotropy, $V$ is the volume of the particle, $k$ is Boltzmann's constant) indicates that ~10 % of the iron atoms are incorporated in the largest particles of diameters $6 < d < 9$ nm. As shown by different methods in a great number of papers (for a selected list, see Ref. 24), the size of the primary particles of iron hydroxide precipitated from solutions with excess alkali is always ~3 nm. In view of this fact, we may infer that the remaining ~90 % of the iron atoms are incorporated in particles, whose diameters vary in the range $3 < d < 6$ nm, and the ratio of the maximum diameter to the minimum diameter $d_{max}/d_{min} \leq 3$.

The Mössbauer spectra of the hydrated sorbent recorded in various velocity viewing windows at room temperature are shown in Fig. 4. With bound diffusion one should expect a characteristic spectrum, which is a superposition of elastic (nonbroadened) and quasielastic (broadened) components. However, a quadrupole doublet with Lorentzian-shaped lines without any signs of diffusion broadening was actually observed. The relatively great width of the line ($\Gamma = 0.40 \pm 0.05$ mm s$^{-1}$) is of purely structural origin, since it does not differ from those observed for a dry sample over the whole temperature range studied and for a hydrated sample at low temperatures (*i.e.*, when diffusion motions are known not to occur) and is typical of nanoparticles of iron hydroxide in the superparamagnetic or paramagnetic states. The area of the spectrum of the hydrated sample at room temperature proved to be 12.5 times smaller than that for the dry sample. It may be suggested that the spectrum of the hydrated sample contains also a

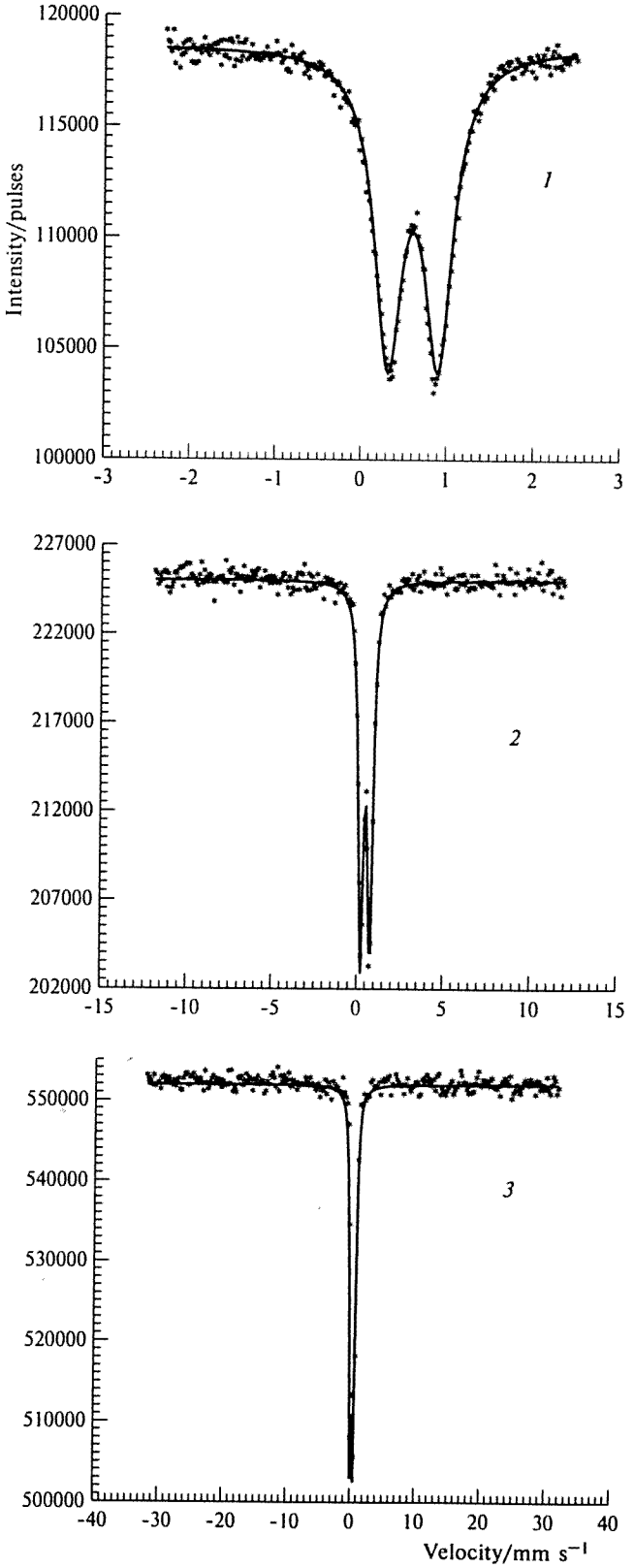


**Fig. 4.** Mössbauer spectra of the hydrated sorbent at 293 K in viewing windows 5 (*1*), 25 (*2*), and 80 (*3*) mm s$^{-1}$.

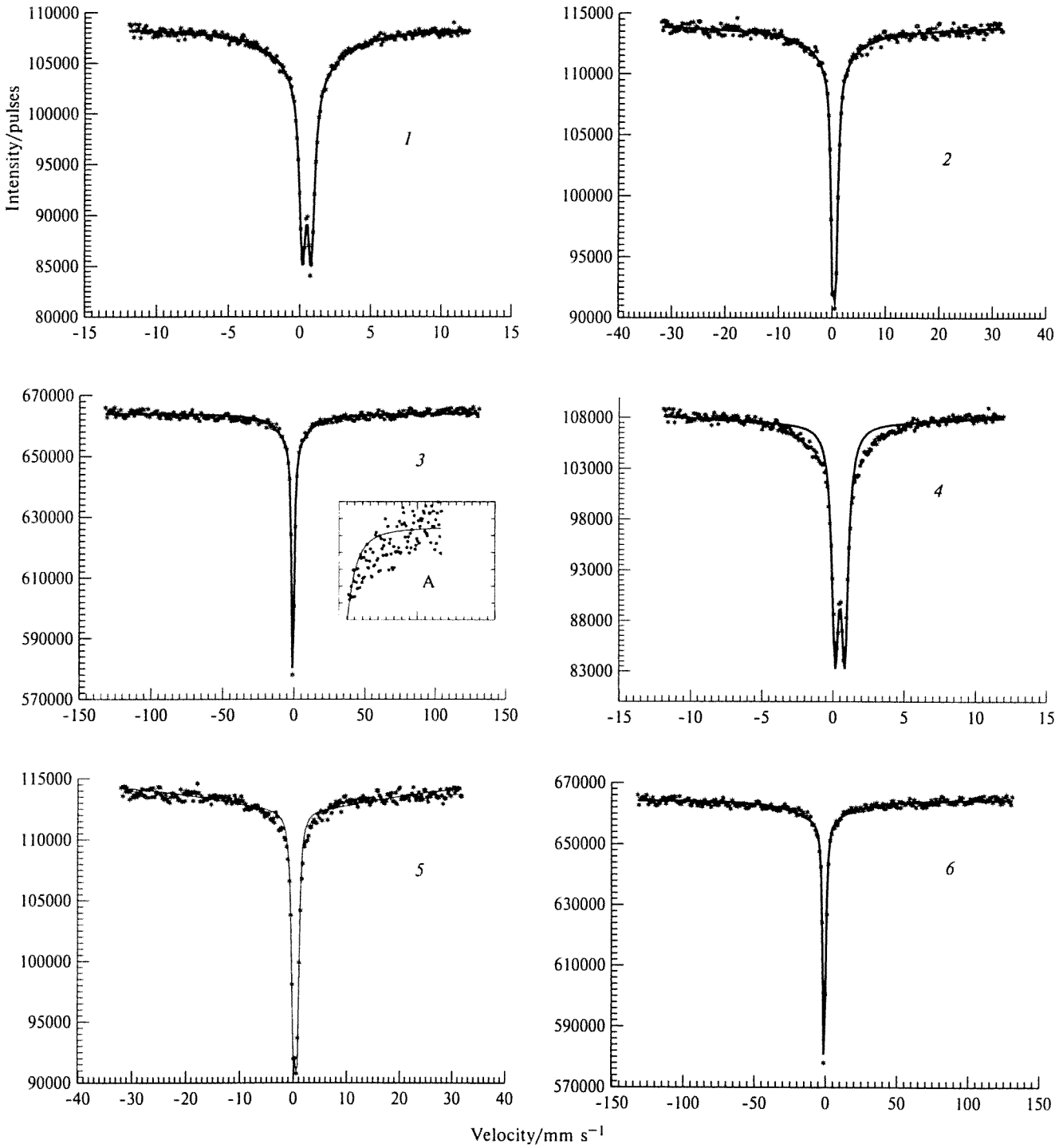


**Fig. 5.** Mössbauer spectra of the sorbent solvated with glycerol at 293 K in viewing windows 25, 80, and 300 mm s$^{-1}$: independent description (*1—3*) for each of the three windows (frame A contains an enlarged fragment with the overall enveloping line) and description with common parameters for all three windows (*4—6*). The continuous line corresponds to the phenomenological description with two Lorentzians.

quasielastic component, but its broadening is so great that it cannot be observed even in the 80 mm s$^{-1}$ velocity window. To verify this suggestion, we replaced the water in the sorbent pores by glycerol, the viscosity of which is ~800 times higher (7.7 P compared to $0.95 \cdot 10^{-2}$ P for water[26]). Consequently, the spectrum assumed the expected form of a superposition of nonbroadened and broadened components normal for bound diffusion (Fig. 5), its area being restored almost completely.

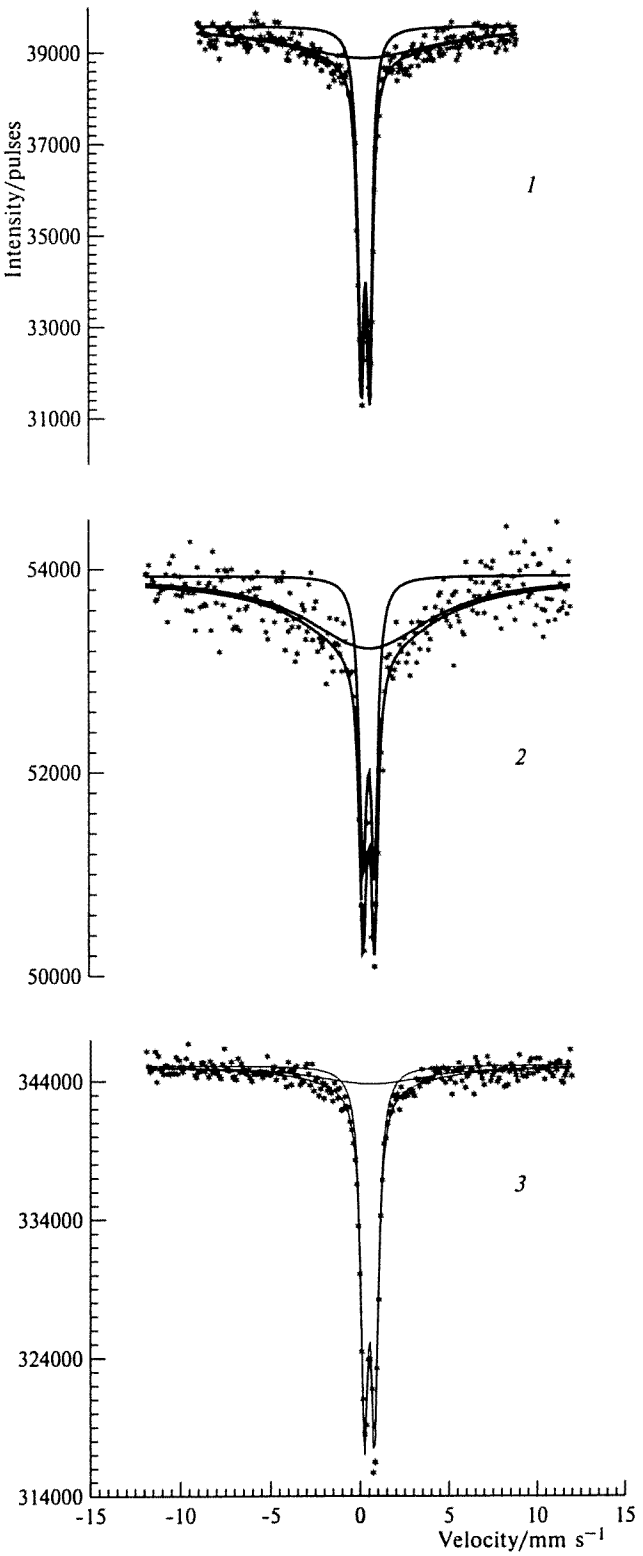


**Fig. 6.** Mössbauer spectra of the hydrated sample at 250 (*1*), 260 (*2*), and 270 K (*3*). Phenomenological description with one broadened Lorentzian.

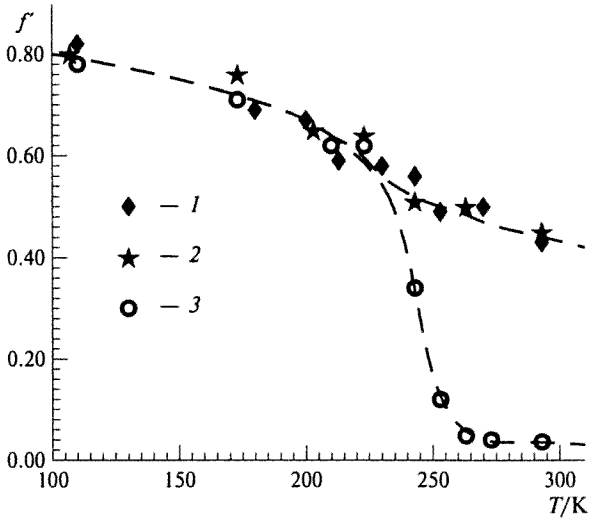


**Fig. 7.** Temperature dependence of the probability of the Mössbauer effect $f$ for dry (*1*), hydrated (*2*), and glycerol (*3*) samples. The $f$ values at $T > 250$ K for the hydrated sample were calculated from the observed areas of the spectrum in the 80 mm s$^{-1}$ window, and those for the glycerol sample were found from the reconstructed overall area in terms of the phenomenological description with two broadened and one nonbroadened Lorentzians.

It was reasonable to try to discover the quasielastic component also in the spectrum of the hydrated sample by decreasing the rate of diffusion, which can be attained by decreasing the temperature. In fact, when a sample quickly frozen in liquid nitrogen was heated, this component appeared at ~250 K (Fig. 6), simultaneously with the beginning of the anomalously abrupt decrease in the area of the spectrum (Fig. 7, curve *3*) (a decrease in the probability of the Mössbauer effect), and was observed up to 270 K. This makes it possible to attribute the additional decrease in the area of the spectrum in the 250—290 K region (with respect to the solid-state dependence $f(T)$ for the dry sample, which is determined by the intraparticle oscillations of atoms) to the fact that, as the temperature increases, the broad component partly and then (at 270—290 K) completely "escapes" the viewing velocity window (in the present case, 80 mm s$^{-1}$), owing to the increase in the rate of the bound diffusion of the particles. In the case of a glycerol sample, broadening of the spectrum was also observed at 250—290 K, but, since the magnitude of the broadening is lower than that for the water-containing sample, the spectrum almost entirely fits in (even at 293 K) the 300 mm s$^{-1}$ window, and no additional decrease (compared to the solid-state behavior $f$) in the observed probability of the Mössbauer effect occurs (see Fig. 7, curves *1* and *2*).

Thus, the particles in the solvated sorbent execute motions of the type of bound diffusion at temperatures above the temperature of defrosting and devitrification of the solvating liquid in the pores. In the general case, the theory predicts the presence of one nonbroadened and a number of broadened Lorentzians in the spec-

trum.[14–17] In the specific case of rather rigid systems with relatively small diffusion displacements, the broadened component can be represented as only one Lorentzian[15] (which has been observed experimentally, for example, for intramolecular mobility of proteins[25] or for the bound diffusion of particles in a solvated polymeric network of an extensively cross-linked cation exchanger[24]).

Therefore, we initially carried out a phenomenological (without a model) description of the spectra of the glycerol sample recorded at room temperature in three viewing windows (30, 80, and 300 mm $s^{-1}$) using one or several broadened Lorentzians and one nonbroadened Lorentzian (naturally, each of them is split into two lines of equal width due to the quadrupole coupling; below, the quadrupole doublets are not mentioned for the sake of simplicity). We found that in the case of one broadened line, this method ensures a good description of the spectra in the 30 and 80 mm $s^{-1}$ windows, but the spectrum in the 300 mm $s^{-1}$ window is poorly described ($\chi^2 \geq 2$ instead of $\chi^2 = 1.00 \pm 0.25$ at a statistically reliable description), which can be seen in Fig. 5, curve *3*. The values obtained for the width of the broadened component in the small, medium, and large windows are completely different: 5.2, 13.1, and 24.7±0.5 mm $s^{-1}$, respectively. The use of common parameters (the widths of both lines and the ratios of their intensities) for the three windows clearly demonstrates (see Fig. 5, curves *4*—*6*) that the interpretation of the spectra with one broadened Lorentzian is inadequate. To carry out a good phenomenological interpretation of all the three spectra using common parameters, no less than three broadened lines are needed. Thus, the broadened component of the spectrum observed by us is a certain set of Lorentzians.

The description of a Mössbauer spectrum under conditions of bound diffusion in terms of the model of the Brownian overdamped oscillator, in which a moving particle is affected by two forces, a quasielastic force (harmonic oscillator) and viscous friction, is well known.[15,16] In this case, the shape of a spectral line in the frequency representation is given by the expression

$$I(\omega) \sim \exp\left(\frac{-k^2 D}{d}\right) \sum_{n=0}^{\infty} \left(\frac{-k^2 D}{d}\right)^n \times \times \frac{1}{n!} \left[\frac{(\Gamma/2 + nd)}{(\omega - \omega_0)^2 + (\Gamma/2 + nd)^2}\right], \quad (1)$$

where $D$ is the diffusion coefficient; $\alpha$ is the ratio of the elasticity and resistance coefficients; $k = 2\pi/\lambda$ is the wave number ($\lambda = 0.86$ Å for $^{57}Fe$); and $\Gamma$ is the natural (instrumental) line width.

A more general approach in which the motion is described as continuous diffusion in a potential of arbitrary form, has also been developed.[17] In terms of this approach, in a study of the dynamics of ultrafine particles in a solvated polymeric network of the polystyrene—divinylbenzene cation exchanger, we were able for the first time to establish the form of the potential in which their motion occurs. It was a three-dimensional analog of the one-dimensional infinitely deep potential well: a sphere of radius $a$ with potential $U(r) = \begin{cases} 0 & r < a \\ \infty & r \geq a \end{cases}$ (from here on, for simplicity, called "rectangular potential"). In this case, the shape of the Mössbauer line is given by the expression[24,28]

$$I(\omega) \sim \frac{A_{00}\Gamma/2}{(\omega - \omega_0)^2 + (\Gamma/2)^2} + + \sum_{n,l}^{\infty} \frac{(2l+1)A_{nl}[\Gamma/2 + D/a^2(\mu_{nl})^2]}{(\omega - \omega_0)^2 + [\Gamma/2 + D/a^2(\mu_{nl})^2]^2}, \quad (2)$$

where $\mu_{nl}$ are the roots of the transcendental equation

$$j_l'(\mu_{nl}) = 0,$$

and $j_l$ are spherical Bessel functions:

$$j_l(Z) = Z^l \left[-\frac{1}{Z}\frac{d}{dZ}\right]^l \frac{\sin Z}{Z}.$$

The intensities of the elastic ($A_{00}$) and quasielastic ($A_{nl}$) components are determined from the relationships

$$A_{00} = \frac{9(ka\cos ka - \sin ka)}{(ka)^6},$$

$$A_{nl} = \frac{6(\mu_{nl})^2}{(\mu_{nl})^2 - l(l+1)} \left[\frac{kaj_{l+1}(ka) - lj_l(ka)}{(ka)^2 - (\mu_{nl})^2}\right]^2.$$

We attempted to describe the spectra observed in terms of both models mentioned above. Two facts indicate the possible anharmonicity of the motions. First, in an arbitrary phenomenological description of the spectra by three or more Lorentzians (one of which is not broadened and is the elastic component), the broadened lines always prove to be nonequidistant in their broadenings, whereas in the Brownian oscillator model, they should be equidistant (harmonic potential). Second, temperature measurements with the glycerol-containing sample have shown that the experimentally observed proportion of the elastic component in the overall area of the spectrum tends to approach a constant value as the temperature increases. The latter is evidence in support of the rectangular potential, because in this model $A_{00}$ does not depend on the temperature, while in the case of a harmonic potential it is temperature dependent.

The model description of the experimental spectra with the use of relationships (1) and (2) did not ensure complete statistical agreement. Moreover, the parameters of the motion obtained from the independent description proved to be different for various windows: the diffusion coefficients ($D \cdot 10^9$) for the rectangular potential are 0.25, 0.50, and 0.9 $cm^2\ s^{-1}$, and those for the harmonic potential are 0.22, 0.5, and 0.65 $cm^2\ s^{-1}$ for the 30, 80, and 300 mm $s^{-1}$ windows, respectively. A description having a physical sense, in which the same

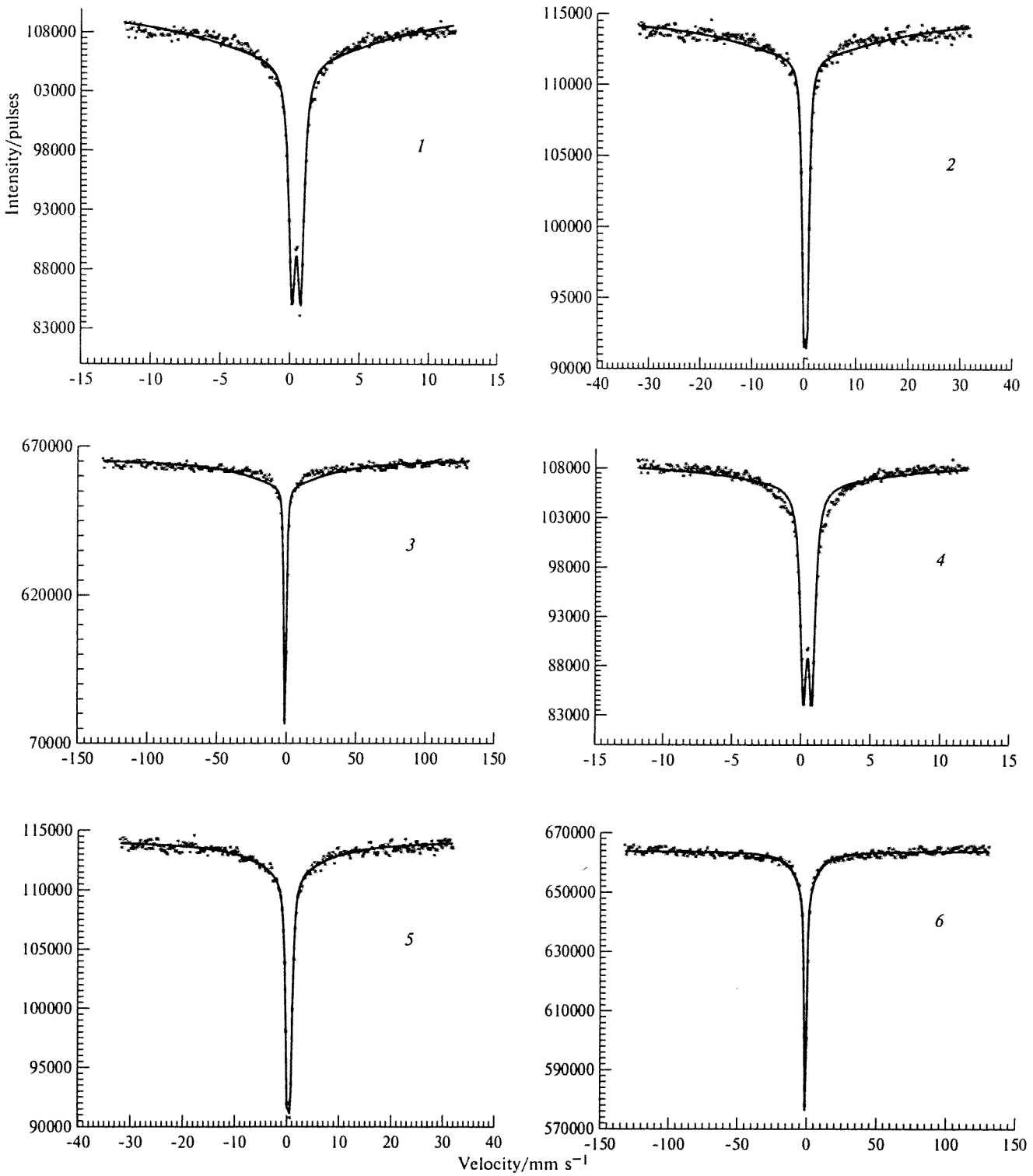


**Fig. 8.** Mössbauer spectra of the sample solvated with glycerol at 293 K in three viewing windows (25, 80, and 300 mm $s^{-1}$): descriptions in terms of the rectangular potential models (*1—3*) and Brownian overdamped oscillator (*4—6*).

parameters are used for all the viewing windows (Fig. 8, curves *1—3* and *4—6*), gives a poorer agreement with experiment. The following values for the parameters of the bound diffusion in the glycerol sample at 293 K were found: for the rectangular potential $D = (0.5\pm0.1)\cdot10^{-9}$ $cm^2$ $s^{-1}$, $r = 0.38\pm0.03$ Å; for the harmonic potential $D = (0.3\pm0.1)\cdot10^{-9}$ $cm^2$ $s^{-1}$, $r = 0.14\pm0.03$ Å.

The above-mentioned discrepancy of the model spectrum with the experimental one may be considered to be quite natural, in view of the fact that the set of particles with appreciably different sizes has been described by common diffusion parameters. An estimate shows that allowance for the difference in the size of particles and, correspondingly, in the coefficients of their diffusion (in a medium with Stokes—Einstein viscosity $\eta$,

$$D = kT/6\pi\eta r) \quad (3)$$

can substantially improve the agreement between the theoretical and experimental line shapes for both models being compared.

It can be readily seen that the spectra in Fig. 8 are better described by Eq. (1) than by Eq. (2). However, one cannot choose between the models under consideration judging from the extent of fit of the theoretical spectrum to the experimental spectrum at one temperature. In order to choose correctly an adequate physical model[17] (one of those used by us or any other), a detailed study of the temperature dependence of the shape of the spectrum in various viewing windows is needed, as has been done previously for another system.[24] Nevertheless, in the present work, we considered it expedient to present the results of a comparison of the two models, strongly differing from each other, in order to demonstrate the degree to which the numerical values of the parameters of the motion under consideration are model-dependent.

The analysis of the areas of the spectra deserves special attention. In the present study, even in the case of glycerol (not to mention water), we are dealing with such great broadenings that the envelope of the spectrum does not reach saturation even in the 300 mm $s^{-1}$ viewing window, which is the most technically accessible to us. If we take into account that the shape of the spectrum is *a priori* unknown, then the only strict value observed experimentally is the area of the part of the spectrum that fits in the viewing window (is confined by the window and by the conventional background line that passes through the intersection of the spectrum envelope with the window border). This observed area $S_{obs}$ (which is naturally smaller than the overall area of the spectrum $S$) is matched by a certain effective probability of the Mössbauer effect $f'_{obs}$, which must be used in the case of very great broadening (we have done this for the hydrated sample; see Fig. 7, curve *3*).

The reconstructed overall area of the spectrum is, naturally, model-dependent and, strictly speaking, it can be found only by increasing the viewing window in the experiment [the largest window in the Mössbauer spectroscopy (1100 mm $s^{-1}$) has been used by us previously[24] in a similar experiment, but the current method of recording makes it possible to achieve ~$10^4$ mm $s^{-1}$].

The question how the overall areas of the spectra recorded in the presence and in the absence of diffusion motions (the glycerol and dry sample, respectively) relate to each other is of principal importance. If all the diffusion motions fit in the reconstructed overall area of the spectrum of the glycerol sample, it should coincide with the area of the spectrum of the dry sample.

The reconstructed overall areas of the spectrum for the glycerol sample at room temperature in the 300 mm $s^{-1}$ window, found in terms of the phenomenological description (using two broadened Lorentzians) and in terms of the model description using Eqs. (1) and (2), are 0.95, 0.45, and 1.03±0.05 of the area of the spectrum of the dry sample, respectively (the observed areas are 0.95, 0.64, and 1.16±0.05, respectively). If we assume that the first and the third variants (the phenomenological description and the description in terms of the rectangular potential model, when the areas of the spectra of the glycerol and dry samples are identical) represent the actual facts, the dynamics of the iron atoms in the glycerol sample is completely reduced to bound diffusion motions of the particles on the whole with the parameters mentioned above and to the solid-state intraparticle atomic oscillations (with an average displacement at room temperature $\langle r^2_{osc}\rangle$ of 0.015 Å$^2$, as determined from the probability of the Mössbauer effect $f' = \exp(-k^2\langle r^2_{osc}\rangle)$. If preference is given to the Brownian oscillator, when the overall area of the spectrum is almost twofold smaller, it is necessary to assume the presence of additional even higher-frequency motions of the particles with a displacement $\langle r^2\rangle$ of 0.012 Å$^2$.

The area of the spectrum of the hydrated sample observed at room temperature (which refers completely to the nonbroadened component) is equal to 0.61 of the area of the nonbroadened line in the spectrum of the glycerol sample. Unfortunately, we were not able to obtain the extrapolated values for the width and area of the broadened component of the spectrum that completely "escaped" at 293 K the widest viewing window used in this case, 80 mm $s^{-1}$, from the low-temperature measurements of the hydrated sample. This is due to the fact that in the 50—270 K temperature range, in which the broadened component is observable, its width in the given window (the simplest phenomenological description of the spectra by one broadened Lorentzian being quite satisfactory) does not depend on the temperature ($\Gamma_{br} \approx 10$ mm $s^{-1}$). This rather obvious artefact is caused by the fact that in the present case, the full spectrum is much wider than the window used (see the phenomenological description of the spectra of glycerol samples in different windows considered above).

It may be suggested that the overall area of the spectrum of the hydrated sample at room temperature (when the broadened component escapes completely the viewing window) is equal to the area of the spectrum of dry sample (as was the case with the glycerol sample in terms of the phenomenological description of the spectrum and of the rectangular potential model). Then the lower limit of the diffusion broadenings corresponding to the experimentally observed spectrum can be easily

estimated by modeling. The simplest estimate based on one broadened Lorentzian affords $\Delta\Gamma \geq 250$ mm $s^{-1}$ and, correspondingly, $D \geq 1.5 \cdot 10^{-8}$ $cm^2$ $s^{-1}$ [from Eq. (4); see below]. From relationship (1), we obtain $D \geq 1.4 \cdot 10^{-8}$ $cm^2$ $s^{-1}$, while Eq. (2) gives $D \geq 2.8 \cdot 10^{-8}$ $cm^2$ $s^{-1}$.

Since, in the variant under consideration, the proportion of the elastic component in the spectrum of the water-containing sample is lower than that for the glycerol sample, the diffusion displacements obtained for the former are correspondingly larger ($r = 0.22 \pm 0.02$ Å in terms of the phenomenological description and the harmonic potential, and $r = 0.45 \pm 0.05$ Å in terms of the rectangular potential). Of course, the alternative variant, when the diffusion displacements in water and glycerol are identical, also cannot be ruled out; but, in this case, the appearance of additional motion modes in the hydrated sample, responsible for the additional 1.5-fold decrease in the overall area of the spectrum (including the elastic component observed), needs to be assumed.

It may be suggested that the rate of the bound diffusion of particles is governed by their interaction with both the liquid and the walls of pores. In this connection, it is of interest to compare the diffusion coefficients obtained by us with the values calculated for the free liquid. Certainly, this comparison is rough for the following reasons: (1) the exact size distribution of the particles is not available, (2) we do not know the viscosity of the liquid in the pores, which should differ from the viscosity of free liquid of the same composition, (3) in the calculation of the viscosity of the water—glycerol mixture in a pore, we neglected the possible selective sorption of one of the components, and (4) a particle can move together with the molecules of the liquid sorbed on it *via* hydrogen bonds, which efficiently increases its radius. Nevertheless, the reasons listed cannot affect too much (by an order of magnitude or more) the quantitative evaluation.

Assuming that the radius of a particle $r$ is 30 Å, we obtain from relationships (3) and (4) (see below) the values for the coefficient $D$ for its diffusion in pure water ($\eta = 0.95 \cdot 10^{-2}$ P) and in glycerol with an admixture of water ($\eta = 7.7 \cdot 10^{-2}$ P), equal to $0.8 \cdot 10^{-6}$ and $1.0 \cdot 10^{-9}$ $cm^2$ $s^{-1}$; respectively; one of these values (for glycerol) is virtually identical to the result found by us from the Mössbauer experiment and the other one (for water) being consistent with it. This estimate indicates that the solvating liquid has a crucial effect on the rate of the bound diffusion of particles. This, in turn, implies that the particles are located in pores, whose sizes are much greater than the sizes of the particles.

Previously we have shown that, for a set of particles of diameter ~30 Å in a solvated polymeric network, a decrease in the size of its cells with the same solvating liquid results not only in a decrease in the diffusion displacements of the particles in the cells, but also in a decrease in the coefficient of their bound diffusion. Thus, in the general case, the contributions of the interactions of a particle with the solid and liquid phases to the rate of its diffusion can be different.

It is natural that a particle, being not chemically bound to the surface of a sorbent pore (since there are no groups that could react with the surface hydroxyls of the particle), is also capable of diffusing infinitely (especially in the case where the barrier to the diffusion over the surface is lower than the adsorption energy), both continuous and jump diffusion being possible. The broadening of the Mössbauer line in the case of unlimited diffusion is known[1,5,6] to be related to the diffusion coefficient. For continuous diffusion:

$$\Delta\Gamma = 2\hbar k^2 D_{cont}, \quad (4)$$

and for jump diffusion (in the long-jump limit $kl \gg 1$)

$$\Delta\Gamma = 12\hbar D_{jump}/l^2, \quad (5)$$

$$\Delta\Gamma = 2\hbar/\tau, \quad (6)$$

where $l$ is the jump length, and $\tau$ is the time of settled life of the atom (in our case, of the particle) between two successive jumps. The absence of broadening in the elastic component of the spectra observed by us for the water- and glycerol-containing samples (with an accuracy of $\Delta\Gamma < 0.1$ mm $s^{-1}$; see Fig. 4) makes it possible, on the basis of Eqs. (4)—(6), to draw the rather important conclusion that unlimited diffusion does not occur to an accuracy of the following magnitudes of the parameters: for continuous diffusion $D_{cont} < 7 \cdot 10^{-12}$ $cm^2$ $s^{-1}$; for jump diffusion $D_{jump}$ [$cm^2$ $s^{-1}$]/$l^2$[$cm^2$] $< 6 \cdot 10^5$ $s^{-1}$ (for example, for $l = 1$ Å $D < 6 \cdot 10^{-11}$ $cm^2$ $s^{-1}$) and $\tau > 3 \cdot 10^{-7}$ s.

It is known that the problem of the interaction of molecules with a solid state surface has been studied in most detail; among other methods, spectroscopy has been used in these studies. The situation with macromolecules and nanoparticles (whose masses are greater by several orders of magnitude) is less clear, and from this viewpoint, the data on the dynamics of these particles on a surface collected by Mössbauer spectroscopy (which is an analog of a sort of vibrational spectroscopy) are of considerable interest. In addition, the interaction of nanoparticles with the surface can serve as a relatively simple model for much more complex systems, such as macromolecules or protein globules, for which the separation of the contributions of their intramolecular motions and their displacements on the whole to the experimentally observed mobility is a rather complex problem, which sometimes lead to inconsistencies in the interpretation of experimental data.[29] Finally, an applied aspect also exists, namely, the possibility of probing the structure of sorbents and ion exchangers by examining the bound diffusion of nanoparticles by Mössbauer spectroscopy, similarly to what is done when NMR and ESR methods are used for recording the motion of molecules, paramagnetic tracers, and probes.

The work was carried out with partial financial support from the Russian Foundation for Basic Research (Project No. 94-03-08081) and the International Science Foundation (Grant No. MOI300).

## References

1. K. S. Singwi and Sjolander, *Phys. Rev.*, 1960, **120**, 1093.
2. P. P. Craig and N. Sutin, *Phys. Rev. Lett.*, 1963, **11**, 460.
3. D. St. P. Bunbury, J. A. Elliott, H. E. Hall, and J. M. Williams, *Phys. Lett.*, 1963, **6**, 34.
4. R. C. Knauer and J. G. Mullen, *Phys. Rev.*, 1968, **174**, 711.
5. J. G. Mullen and R. C. Knauer, in *Mössbauer Effect Methodology*, Ed. I. G. Gruverman, Plenum Press, New York, 1970, **5**, 197.
6. Ch. Janot, *J. Phys. (Paris)*, 1976, **367**, 253.
7. Ch. Janot, *J. Phys. (Paris)*, 1978, Colloque No. 2, Suppl. No. 3, C-2-238.
8. P. A. Flinn, in *Applications of Mössbauer Spectroscopy*, Ed. R. L. Cohen, Academic Press, New York, 1980, **2**, 393.
9. G. Vogl, *Hyperfine Interact.*, 1990, **56**, 197.
10. J. A. Elliot, H. E. Hall, and D. St. P. Bunbury, *Proc. Phys. Soc. (London)*, 1966, **89**, 595.
11. S. L. Kordyuk, V. I. Lisichenko, O. L. Orlov, N. N. Polovina, and A. N. Smoilovskii, *Zh. Eksp. Teor. Fiz.* [*J. Exp. Theor. Phys.*], 1967, **52**, 611 (in Russian).
12. K. P. Singh and J. G. Mullen, *Phys. Rev., A*, 1972, **6**, 2354.
13. H. Keller and W. Kundig, *Solid State Commun.*, 1975, **16**, 252.
14. M. A. Krivoglaz and S. P. Repetskii, *Fiz. Tverd. Tela* [*Solid-State Physics*], 1966, **8**, 2908 (in Russian).
15. I. Nowik, S. G. Cohen, E. R. Bauminger, and S. Ofer, *Phys. Rev. Lett.*, 1983, **19**, 1528.
16. I. Nowik, E. R. Bauminger, S. G. Cohen, and S. Ofer, *Phys. Rev., A*, 1985, **31**, 2291.
17. A. M. Afanas'ev and V. E. Sedov, *Phys. Status Solidi (b)*, 1985, **131**, 299.
18. A. Blasius, R. S. Preston, and U. Gonser, *Z. Phys. Chem. Neue Folge*, 1979, **195**, 187.
19. W. Petry, G. Vogl, and W. Mansel, *Phys. Rev. Lett.*, 1980, **45**, 1862.
20. S. Morup, A. M. Afanas'ev, and P. V. Hendriksen, *Hyperfine Interact.*, 1994, **88**, 3548.
21. A. M. Afanas'ev, L. V. Bashkeev, A. S. Plachinda, V. E. Sedov, and V. I. Khromov, *Khim. Fiz.* [*Chem. Phys.*], 1989, **8**, 986 (in Russian).
22. A. S. Plachinda, V. E. Sedov, V. I. Khromov, L. V. Bashkeev, and I. P. Suzdalev, *Chem. Phys. Lett.*, 1990, **175**, 101.
23. G. U. Nienhaus, A. S. Plachinda, M. Ficher, V. I. Khromov, F. Parak, I. P. Suzdalev, and V. I. Goldanskii, *Hyperfine Interact.*, 1990, **56**, 1471.
24. A. S. Plachinda, V. E. Sedov, V. I. Khromov, I. P. Suzdalev, V. I. Goldanskii, G. U. Nienhaus, and F. Parak, *Phys. Rev., B*, 1992, **45**, 7716.
25. E. W. Knapp, S. F. Fischer, and F. Parak, *J. Chem. Phys.*, 1983, **78**, 4701.
26. J. Timmermans, *The Physicochemical Constants of Binary Systems in Concentrated Solutions*, Interscience, New York, 1960, **4**, 309.
27. B. Rodmacq, *J. Phys. Chem. Solids*, 1984, **45**, 1119.
28. F. Volino and A. J. Dianoux, *Mol. Phys.*, 1980, **41**, 271.
29. V. N. Morozov and T. Yu. Morozova, *J. Theor. Biol.*, 1986, **121**, 73.

*Received May 31, 1995;*
*in revised form November 3, 1995*